Journal of Cellular Physiology

Shear Flow-Induced Formation of Tubular Cell Protrusions in Multiple Myeloma Cells

ZIV PORAT,[1] ITAMAR YARON,[1] BEN-ZION KATZ,[2] ZVI KAM,[1] AND BENJAMIN GEIGER[1]*

[1]Department of Molecular Cell Biology, Weizmann Institute of Science, Rehovot, Israel

[2]Hematology Institute, Tel Aviv Sourasky Medical Center and Sackler Faculty of Medicine, Tel Aviv University, Tel Aviv, Israel

Exposure of live cells to shear flow induces major changes in cell shape, adhesion to the extracellular matrix, and migration. In the present study, we show that exposure of cultured multiple myeloma (MM) cells to shear flow of 4–36 dynes/cm^2 triggers the extension of long tubular protrusions (denoted flow-induced protrusions, or FLIPs) in the direction of the flow. These FLIPs were found to be rich in actin, contain few or no microtubules and, apart from endoplasmic reticulum (ER)-like membranal structures, are devoid of organelles. Studying the dynamics of this process revealed that FLIPs elongate at their tips in a shear force-dependent manner, and retract at their bases. Examination of this force dependence revealed considerable heterogeneity in the mechanosensitivity of individual cells, most likely reflecting the diversity of the malignant B cell population. The mechanisms underlying FLIP formation following mechanical perturbation, and their relevance to the cellular trafficking of MM cells, are discussed.

J. Cell. Physiol. 226: 3197–3207, 2011.

Living cells are highly sensitive to external cues, delivered to them via the surrounding environment, including the chemical nature of the extracellular matrix (ECM) and its physical properties (Juliano, 1996; Discher et al., 2009; Heino and Kapyla, 2009). Recent studies have indicated that cells are capable of sensing multiple features of such external surfaces, including their rigidity (Discher et al., 2005; Engler et al., 2006; Moore et al., 2010), micro-topography (Curtis and Riehle, 2001; Spatz and Geiger, 2007; Geblinger et al., 2010), anisotropy (Thery et al., 2006), dimensionality (Cukierman et al., 2001; Doyle et al., 2009), and mechanical activity (Bershadsky et al., 2003; Vogel and Sheetz, 2006; Chen, 2008). These stimulations can activate a wide variety of global cellular responses, such as regulation of cell proliferation, differentiation, and survival (Nelson et al., 2005; Kurpinski et al., 2006; Vogel and Sheetz, 2006), as well as local responses, manifested by alterations in cell shape and polarization (Chen et al., 1997; Vogel and Sheetz, 2006), directional migration (Friedl and Wolf, 2010; Van Goethem et al., 2010), and reorganization of ECM adhesions (Cohen et al., 2004; Zaidel-Bar et al., 2004; Fouchard et al., 2011; Papusheva and Heisenberg, 2010).

A vast body of knowledge on cellular mechanosensitivity has accumulated by tracking cell behavior during exposure to shear flow. Thus, exposure of endothelial cells to shear forces of 5–15 dynes/cm^2 affects cell morphology, lamellipodial protrusions, and cell migration (Dewey et al., 1981; Masuda and Fujiwara, 1993; Galbraith et al., 1998; Wojciak-Stothard and Ridley, 2003; Zaidel-Bar et al., 2005). Leukocytes subjected to shear flow undergo major morphological changes, transforming from a spheroid shape in the circulation into a flat, adherent form on the endothelium, and then into an amoeboid morphology while migrating within the target tissues (Dong et al., 1999; Cinamon et al., 2001; Simon and Goldsmith, 2002; Alon and Dustin, 2007; Stroka and Aranda-Espinoza, 2010).

These and additional studies, demonstrating the effects of shear stress on cells, raised the possibility that cellular mechanosensitivity might particularly affect the trafficking of multiple myeloma (MM) cells, a malignancy of terminally differentiated B cells (Kyle and Rajkumar, 2004; Ludwig et al., 2010). MM cells undergo complex differentiation and selection processes in secondary lymphoid organs. Currently, the primary transforming events leading to the development of MM are unclear; yet the transformed plasma cells can evolve into several types of malignant disease, designated plasma cell dyscrasias (Sher et al., 2010). One of the primary differences between the various types of plasma cell dyscrasia is their pathological presentation, which is affected by the tissue organization of the cells. On one hand, solitary plasmacytomas are characterized by the localized, dense (often extramedullary) outgrowth of plasma cells, in a manner similar to metastases originating in solid tumors. On the other hand, plasma cell leukemia is characterized by the continuous presence of malignant plasma cells in the circulation, as well as in the bone marrow (BM), as seen in different types of acute leukemias (e.g., AML, ALL). In contrast, the vast majority of patients with plasma cell dyscrasias are diagnosed with MM, which is considered a systemic disease (Kumar, 2010). MM is characterized by the restricted growth of malignant plasma cells in the BM, but typically involves multiple growth lesions in patients. This unique dissemination pattern most likely involves the exit of MM cells from the BM niche, where they initially evolve, into the circulation, followed by their homing back to the BM (Van Camp and Van Riet, 1998; Vande Broek et al.,

Abbreviations: MM, multiple myeloma; BM, bone marrow; FLIP, flow-induced protrusion

Z. Porat and I. Yaron contributed equally to this work.

Supporting information may be found in the online version of this article.

Contract grant sponsor: National Institutes of Health (NIH) Common Fund, Nanomedicine Program;
Contract grant number: PN2 EY 016586.
Contract grant sponsor: The NanoII Project, supported by the EU FP7 program;
Contract grant number: 229289.

*Correspondence to: Benjamin Geiger, Department of Molecular Cell Biology, Weizmann Institute of Science, Rehovot 76100, Israel.
E-mail: benny.geiger@weizmann.ac.il

Received 8 November 2010; Accepted 28 January 2011

Published online in Wiley Online Library (wileyonlinelibrary.com), 22 February 2011.
DOI: 10.1002/jcp.22680

2008). During this process, the cells move from a low-shear environment (in the BM) to one of high shear (the bloodstream), and back to the BM. The possible consequences of these radical transitions are intriguing.

To investigate the response of MM cells to changes in shear flow, we microscopically monitored the shape and behavior of several MM cell lines, following exposure to shear stress. We found that shear stress of >4 dynes/cm^2 induces cell alignment, and the extension of long tubular protrusions, which we named flow-induced protrusions (FLIPs). Time-lapse monitoring of FLIP extension indicated that the number of FLIP-forming cells, and the average delay between application of flow and the onset of FLIP extension, are proportional to the degree of shear stress. We further show that FLIPs elongate at their tips and retract at their bases, displaying a net growth rate of about 5 μm/min. Long-term exposure to relatively high (>20 dynes/cm^2) shear forces attenuated FLIP extension. The mechanisms underlying FLIP formation, and their possible physiological roles, are discussed.

Materials and Methods

Chemicals and reagents

Fibronectin, Triton X-100, anti-α-tubulin antibodies, and phalloidin-FITC were purchased from Sigma (St. Louis, MO). Streptomycin, penicillin, and glutamine were purchased from Biological Industries (Kibbutz Beit Haemek, Israel). Fetal bovine serum was purchased from Hyclone (South Logan, UT). The fluorescent dye carboxyfluorescein succinimidyl ester (CFSE) was purchased from Molecular Probes (Invitrogen, Carlsbad, CA). RPMI medium was purchased from Gibco (Carlsbad, CA). Tissue culture plates were purchased from Corning (Acton, MA).

Cell cultures

The ARH-77, EBV-transformed plasma cell line was kindly provided by Hanna Ben-Bassat (Hadassah Medical School, Jerusalem, Israel) (Gooding et al., 1999; Nadav et al., 2006). The MM cell lines RPMI 8226 and CAG were received from M. Lischner (Meir Medical Center, Kfar Saba, Israel). Unless otherwise stated, cells were cultured in RPMI medium supplemented with 2 mM glutamine, 50 μg/ml streptomycin, 50 U/ml penicillin, and 20% heat-inactivated bovine serum at 37°C in a humidified incubator, in an atmosphere of 5% CO_2 and 95% air.

Production and maintenance of adhesive subpopulations of ARH-77 cells

The adhesive (type A) and nonadhesive (type F) subpopulations of the ARH-77 cell line were produced, as previously described (Nadav et al., 2006). Briefly, ARH-77 cells were plated on fibronectin-coated (15 μg/ml) tissue culture plates. Cells were left to adhere for 2–3 days; adherent and nonadherent cells were then separated, and replated onto new fibronectin-coated plates. The same process was repeated twice a week for 6 weeks, until two phenotypes—one stable, highly adhesive and the other, stable, poorly adhesive—were established. The two subpopulations were routinely maintained on fibronectin-coated plates, to preserve the unique characteristics of each subline.

Flow chamber apparatus

A parallel plate flow chamber (GlycoTech, Rockville, MD) was assembled according to the manufacturer's instructions, and fixed to the microscope stage using a custom-made Perspex holder (see Supplementary Diagram 1). An upper reservoir containing 50 ml of serum-free medium was connected by a tube to the chamber, which was drained into a lower reservoir. The height difference between the reservoirs created a gravity-driven flow from the upper to the lower reservoir through the flow chamber. A peristaltic pump (Minipuls 3; Gilson, Middleton, WI) was used for pumping medium from a large reservoir containing 400 ml of warm medium, to the upper reservoir, to maintain a constant level of medium. For the flow experiments, 1.25×10^6 ARH-77 type A cells were plated on 35 mm round number 1 coverslips (Marienfeld Laboratory Glassware, Lauda-konigshofen, Germany). After the indicated incubation time, the coverslip was inserted into the flow chamber. The flow rate was controlled by changing the height difference between the two reservoirs, and the shear stress, τ, was calculated (in dynes/cm^2) from the measured volumetric flow rate (Q; ml/sec), using the equation $\tau = 6\eta Q/a^2 b$, where η is the apparent viscosity of the medium (taken to be 0.76 cP); a, channel height (0.025 cm); and b, channel width (0.5 cm). The flow medium was RPMI1640 without addition of serum; the pH and temperature were controlled and monitored. A constant temperature of 37°C was maintained by placing the chamber in a 37°C temperature-controlled box with a liquid heater inside. A custom-made bubble trap was added to assure smooth medium flow, and a special valve was installed at the entry point of the chamber, to enable the rapid introduction of chemical fixatives while maintaining a constant shear flow.

Transmission electron microscopy of cell cultures

Cells were subjected to flow (as indicated) for 20 min, and then fixed for 5 min, under flow, in Karnovsky fixative (2% gluteraldehyde, 3% paraformaldehyde, and 3% sucrose, in 0.1 M cacodylate buffer, pH 7.2). They were then fixed in the same fixative for 2.5 h without flow at room temperature, washed four times in 0.1 M cacodylate buffer, and kept at 4°C until further processing. Cells were post-fixed with 1% OsO_4, 0.5% $K_2Cr_2O_7$, 0.5% $K_4[Fe(CN)_6]\cdot 3H_2O$, 3% sucrose in 0.1 M cacodylate buffer for 2 h at room temperature, and washed twice with 0.1 M cacodylate buffer, 3% sucrose, and three times with double distilled water (DDW). Cells were then stained with 2% uranyl acetate for 1 h, washed with DDW, dehydrated in ethanol, and embedded in Epon—EMBED 812 (EMS, Hatfield, PA). The Epon blocks were then rough-cut into small pieces, aligned according to the flow direction, and re-embedded. Finally, frontal 70–100 nm ultra-thin sections were cut with a Leica ultracat UCT ultramicrotome, and analyzed in a C-12 FEI electron microscope; images were taken with an Eagle 2k × 2k CCD camera.

Scanning electron microscopy

Cells were seeded, fixed and washed on 12 mm round glass coverslips as described above, dehydrated in ethanol, and critical point-dried with a Baltek CPD 030 apparatus (Baltek, Northvale, NJ). The coverslips were then sputtered with gold (Sputter Coater, S150 Edwards, Crawley, UK), and observed with a scanning electron microscope (SEM Ultra 55, Zeiss, Peabody, MA).

Immunostaining and fluorescence microscopy

Cells were simultaneously fixed and permeabilized under flow, with a mixture of 3% paraformaldehyde in PBS, 0.25% Triton X-100, and 0.2% glutaraldehyde, followed by an additional 20 min of incubation without flow. Prior to staining, cells were treated with ~1 mM sodium borohydride in PBS, to reduce autofluorescence. After fixation, cells were washed with PBS and labeled for α-tubulin (1:500, DM1A, Sigma) and actin (phalloidin–FITC; 1:350, Sigma). The nucleus was stained with DAPI (1:2,000, Sigma). Fluorescence and phase-contrast images were acquired with a DeltaVision system (Applied Precision, Inc., Issaquah, WA) equipped with an Olympus IX71 inverted fluorescence microscope and a CCD camera (Cool SNAP HQ^2, Photometrics, Tucson, AZ).

Time-lapse microscopy

To visualize the dynamic behavior of myeloma cells under flow, time-lapse microscopy was used. Suspended ARH-77 type A cells were washed in serum-free medium, stained with the cytoplasmatic fluorescent dye CFSE for 10 min, washed with

growth medium, and then seeded and placed in the apparatus, as described above. Fluorescent and phase-contrast time-lapse movies of cells in the flow apparatus were acquired with 10×/0.3, 20×/0.5, or 40×/0.75 objectives for varying lengths of time (10–120 min) at 10 or 12 sec intervals, as indicated.

Image analysis

"FLIP" formation analysis. FLIP formation analysis was carried out in two steps: automatic cell segmentation, followed by FLIP manual identification. Fluorescent images of CFSE-loaded cells were pre-processed, using a high-pass filter to reduce noise, and a low-pass filter to correct for uneven illumination. Segmentation and creation of binary cell masks were based on seeded watershed (Zamir et al., 1999). Object-by-object, multi-parametric datasets were saved for each image in separate files, enabling continuous tracking of individual cell parameters throughout the image sequence. User-controlled ranges (minimum to maximum) defined the objects to be included in the dataset and excluded outliers, such as wrongly tracked cells and multi-cell clusters.

Results

Induction of long tubular protrusions in cultured MM cells by shear flow

Exposure of cultured ARH-77 type A cells (the adhesive MM cell line), to a shear flow of 4–36 dynes/cm^2, induces major changes in the shape of the treated cells, manifested by the extension of long, tubular protrusions (typically, 2 μm in diameter and ~10–20 μm in length) in the direction of the flow (Fig. 1B; compare to the same cells prior to application of shear flow in Fig. 1A; see also Supplementary Movie 1). Based on their shape and flow dependence, we termed these protrusions, "FLIPs". There was no major change in the cells' aspect ratios, yet in ~75% of the cells exposed to the flow, the major axis was aligned parallel to the flow direction.

The formation of FLIPs was not exclusive to the ARH-77 cells, but was also observed in other adherent MM cell lines (e.g., CAG and RPMI8226; see Supplementary Fig. 1A–D), and when plated on a cultured endothelial monolayer (Supplementary Fig. 1E). On the other hand, FLIP-like structures were not induced in a wide variety of other cell types (including HeLa, H1299, MDA-231, and RAW 264.7) following shear treatment, nor in stationary MM cells. Thus, this phenomenon appears to be flow-dependent, and cell-type specific.

Examination of shear-treated and untreated ARH-77 type A cells by scanning electron microscopy indicated that flow-induced cell polarization was manifested by the formation of a "matrix anchoring zone" at the edge of the cells facing the external flow (Fig. 2B,C, arrowheads) and an accumulation of microvilli and filopodia at the cells' edge, pointing in the direction of flow. These membrane protrusions were dominated, in up to ~40% of the cells, by one large FLIP (Fig. 2B–D), connected to the cell body via a narrow "neck."

Transmission electron microscopy (TEM) of Epon sections, cut along or across FLIPs, indicated that these protrusions are largely devoid of cytoplasmic organelles (Fig. 3), but highly enriched with sub-membrane microfilaments, which were most conspicuous at the neck of the FLIP (Fig. 3B1, arrowhead). Occasionally, stacks of membrane inclusions, resembling endoplasmic reticulum (ER), were detected in the FLIPs' core (Fig. 3B2, arrowheads). Notably, similar membrane arrays were prominent throughout the cytoplasm of MM cells, in both stationary and shear-stressed cultures (data not shown).

The cytoskeletal association with FLIPs in ARH-77 type A cells was further studied by 3D fluorescence microscopy examination of actin and tubulin. In stationary cells (Fig. 4, parts A,B), the organization of actin relative to the major cell axis was apparently random; microtubules were highly enriched in the perinuclear area, with occasional microtubules extending into lamellar or filopodial protrusions. The microtubule organizing center in these cells was usually located above ("dorsal" to) the nucleus, and showed no apparent spatial relationships to the lamellipodia or filopodia.

Upon application of shear flow (20 dynes/cm^2 for 10 min), a radical change in actin and tubulin organization was observed. This was manifested by reduction of lamellipodial and filopodial extensions, and formation of a single, F-actin-rich "dominant" FLIP. Staining with fluorescent phalloidin indicated that F-actin was primarily localized along the FLIP's membrane, in line with TEM observations. The microtubule system, on the other hand, became less organized following the application of shear flow, with only occasional intrusion of microtubules into the FLIP, and with no correlation between the orientation of the FLIP and the centrosome (Fig. 4, parts C,D). Three-dimensional reconstruction (Supplementary Movie 2) of F-actin, microtubules, and nuclei in stationary and flow-treated cells, confirmed these observations, and indicated overall cell rounding following flow treatment, and a clear separation between the FLIP and the underlying substrate.

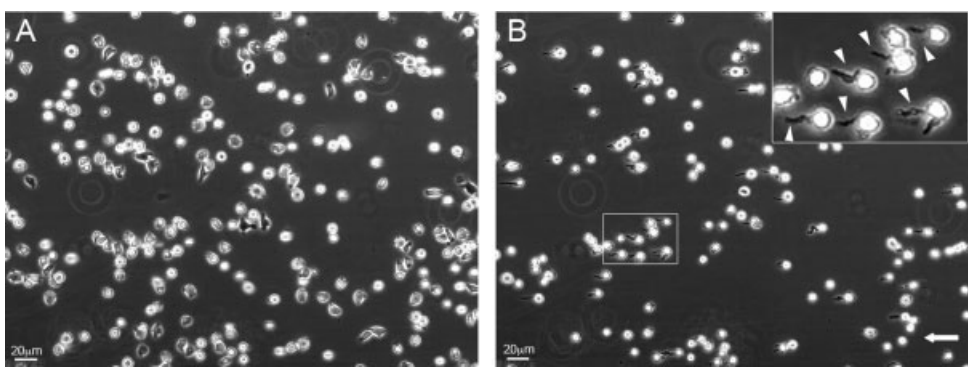

Fig. 1. ARH-77 type A multiple myeloma cells develop tubular protrusions (FLIPs) upon exposure to shear flow of >10 dynes/cm^2. Cells were seeded and allowed to adhere to fibronectin-coated glass coverslips, placed in a flow chamber, and exposed to shear flow. Shown are phase-contrast images of (A) cells under stationary conditions; and (B) cells under shear flow of 20 dynes/cm^2, for 8 min, forming numerous FLIPs. The inset shows a magnification of the marked area. White arrowheads point to induced FLIPs. Direction of flow is indicated by the arrow.

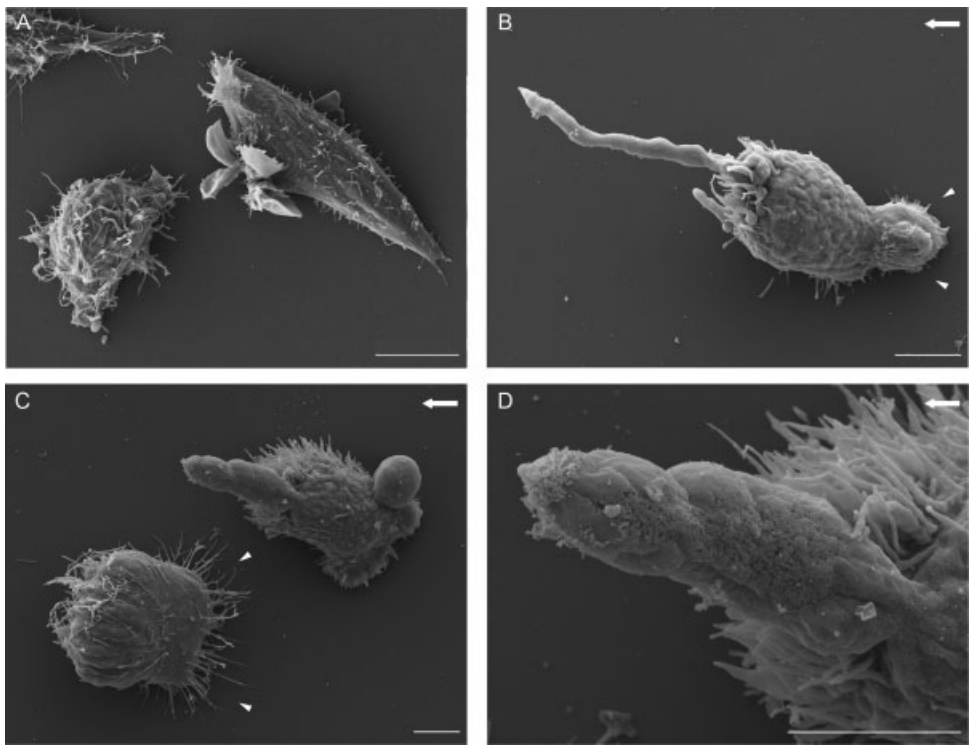

Fig. 2. The FLIP is a narrow tubular protrusion with a typical length of up to 20 μm, extending in the direction of flow. Scanning electron microscope images of ARH-77 type A cells under flow. Cells were fixed under flow, and processed for electron microscopy. A: Control cells, not exposed to flow, showing numerous villi and lamellae on their entire surface. B, C: Cells under flow (20 dynes/cm^2), showing the formation of "matrix anchoring zones" at the edges of the cells, facing the external flow (arrowheads) and reduction in surface microvilli and lamellae. All membrane protrusions localize to the end of the cell, in the direction of the flow. D: Higher-magnification image of the FLIP shown in (C). The direction of flow is indicated by an arrow. Scale bars are 5 μm.

Disruption of microtubules by nocodazole neither reduced nor enhanced FLIP formation (data not shown), supporting the notion that the integrity of the microtubular system is not essential for FLIP formation. The role of F-actin in FLIP formation could not be assessed, since drugs affecting actin polymerization or actomyosin contractility reduced cell adhesion to the substrate, and induced massive cell detachment upon exposure to flow of 4 dynes/cm^2 or higher.

Dynamics of FLIP extension and retraction

Temporal analysis based on live cell microscopy indicated that FLIPs elongate predominantly at their tips, similar to the protrusion of the leading edge of migrating cells (Mitchison and Cramer, 1996). The formation and retraction of a single FLIP (both taking place under continuous shear stress of 20 dynes/cm^2) is shown in Figure 5 and Supplementary Movie 3, and based on a representative 6-min movie. Examination of the location of fiduciary irregularities along the FLIP relative to the FLIP's tip or base, indicated that FLIP elongation involved two simultaneous, yet apparently conflicting processes: tip extension, and base retraction. Under flow, the rate of tip extension greatly exceeded that of base retraction, as indicated by the dashed line in Figure 5. Within a timespan of 0–170 sec, the average tip extension rate was ~7 μm/min, and the base retraction rate was ~2 μm/min, resulting in an average elongation rate of about 5 μm/min. During the retraction phase (Fig. 5, 180–350 sec), tip extension was completely arrested, while the base retraction persisted, and even accelerated (typically, ~4 μm/min). Further experiments performed with other MM cell lines indicated that the elongation–retraction response to shear flow was nearly identical to that of ARH-77 cells. Thus, the average elongation rate for of FLIPs formed by CAG cells was 5.6 μm/min, and the retraction rate was 4.6 μm/min.

Force- and time dependence of FLIP formation

What is the mechanism underlying mechanical stimulation of FLIP formation? To gain insights into this process, fibronectin-adherent ARH-77 MM type A cells were subjected for 40 min to different levels of shear stress, within the range of 4–36 dynes/cm^2; the number of FLIP-forming cells was determined by time-lapse video microscopy. Specifically, we quantified the percentage of FLIP-bearing cells detected at different time points for each shear level, the cumulative percentage of cells that produced FLIPs throughout the incubation time, and the number of FLIP extension and retraction events.

Exposure of the cells to a shear flow of 4 dynes/cm^2 induced FLIP formation that reached a maximum value of 5% FLIP-bearing cells following 10–13 min of treatment; this value persisted for an additional 30 min (Fig. 6). No FLIP formation was observed following exposure to forces lower than 4 dynes/cm^2. Treatment of cells with increasing shear levels (12, 20, 28, and 36 dynes/cm^2) resulted in a greater percentage of responding cells, up to 35–40%, and a narrower interval between application of shear force, and reaching that plateau (Fig. 6). FLIPs formed more rapidly under conditions of stronger shear flow, as shown here for the first 2 min following application of force (Fig. 6, inset). It is noteworthy that the cumulative percentage of cells that ever produced a FLIP in

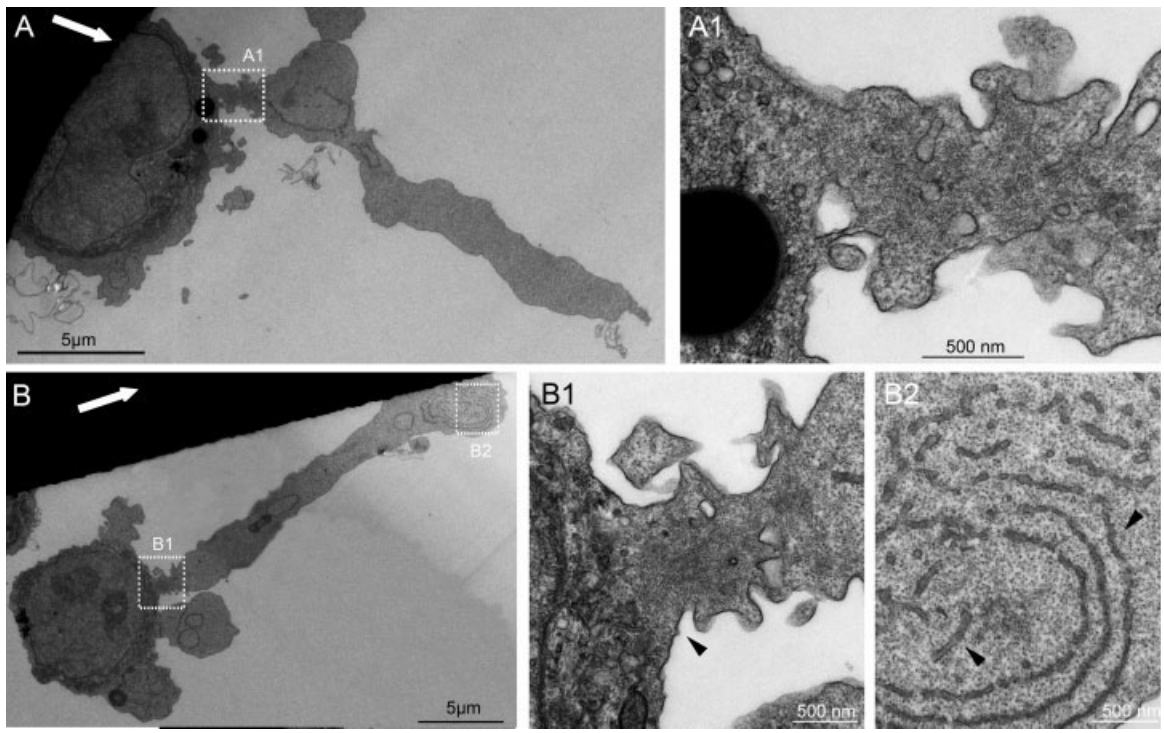

Fig. 3. Transmission electron microscopy images of FLIP-forming cells. ARH-77 type A cells were fixed under flow, and processed for electron microscopy. A, B: Examples of two cells under flow. Flow direction is denoted by the white arrows. A1: Enlargement of the area marked in (A). B1, B2: Higher magnification of the marked areas in (B). FLIPs are mostly devoid of organelles. B1: The FLIP "neck," marked by arrowhead, contains microfilaments. B2: FLIPs often contain ER-like membranal structures, marked with arrowheads.

these experiments was significantly higher than that shown in Fig. 6, reaching up to ~60% under shear levels higher than 20 dynes/cm^2. This finding suggests that the cell population we studied is heterogeneous in its responsiveness to mechanical stimulation (as manifested by FLIP formation). It is also noteworthy that cells treated with the highest shear levels (28 and 36 dynes/cm^2) reached maximum FLIP values within a few minutes, and then declined to about 15%, suggesting that long exposure to shear stress can suppress the mechanical responsiveness of the cells. Interestingly, analysis of FLIP extension and retraction events indicated that increased force facilitated FLIP extension, but had no impact on the frequency of FLIP retraction (Fig. 7).

These results, illustrated in Figure 6, indicate that individual MM cells differ in their mechanosensitivity, and that exposure to flow can eventually suppress force-induced FLIP formation. This suppression could, however, be attributed to either force- or time-dependent downregulation of FLIP formation. To distinguish between these possibilities, ARH-77 cells were subjected to a stepwise increase in shear stress, starting with 4 dynes/cm^2, and followed by seven increments of 4 dynes/cm^2 each. The duration of each step varied from 1 to 8 min. The entire process, including FLIP formation, was continuously monitored microscopically.

The results presented in Figure 8 indicate that FLIP suppression is induced by shear flow, yet is highly dependent on the duration, rather than the force, of the shear. Thus, when the force was increased in 1- or 2-min increments, the percentage of FLIP-producing cells increased steadily until reaching the maximum level, in which ~25% of the cells produced FLIPs (Fig. 8). On the other hand, when the force was increased over a longer timespan, the percentage of FLIP-producing cells did not surpass 15%, supporting the notion that the duration of the exposure to flow plays a key role in the suppression process. These results are in agreement with the "adaptation timeframe" shown in Figure 6, in which the FLIP-forming cells reach a value of ~15% following long incubation periods under shear flow conditions, regardless of the force applied. This finding further indicates that the MM cells are heterogeneous, not only in their mechanosensitivity threshold, but also in their tendency to undergo long-term adaptation to the flow. It is interesting to note that despite showing a lower percentage of responding cells, the force response profile of the CAG cell line was very similar to the ARH-77 type A cells (Supplementary Fig. 4).

Single-cell variations in FLIP production reflect heterogeneous mechanosensitivity in the MM cell population

The experiments described above point up the complexity of the processes underlying the regulation of shear-induced FLIP formation, manifested by variable mechanical thresholds in different cells; and the control of FLIP dynamics, including the balance between FLIP extension and retraction, FLIP lifespan, time intervals between FLIP formation events, and shear-induced FLIP suppression. To gain insights into the inter-relationships between these diverse manifestations of the mechanical response, we performed single-cell analysis of FLIP formation and retraction under different levels of shear force. Examination of the FLIP lifespan upon exposure to varying degrees of force revealed that the cells can be roughly divided into two subpopulations (Fig. 9): "Fast-retracting" cells that retain their FLIPs for up to 12 min (~60% of the cells), and

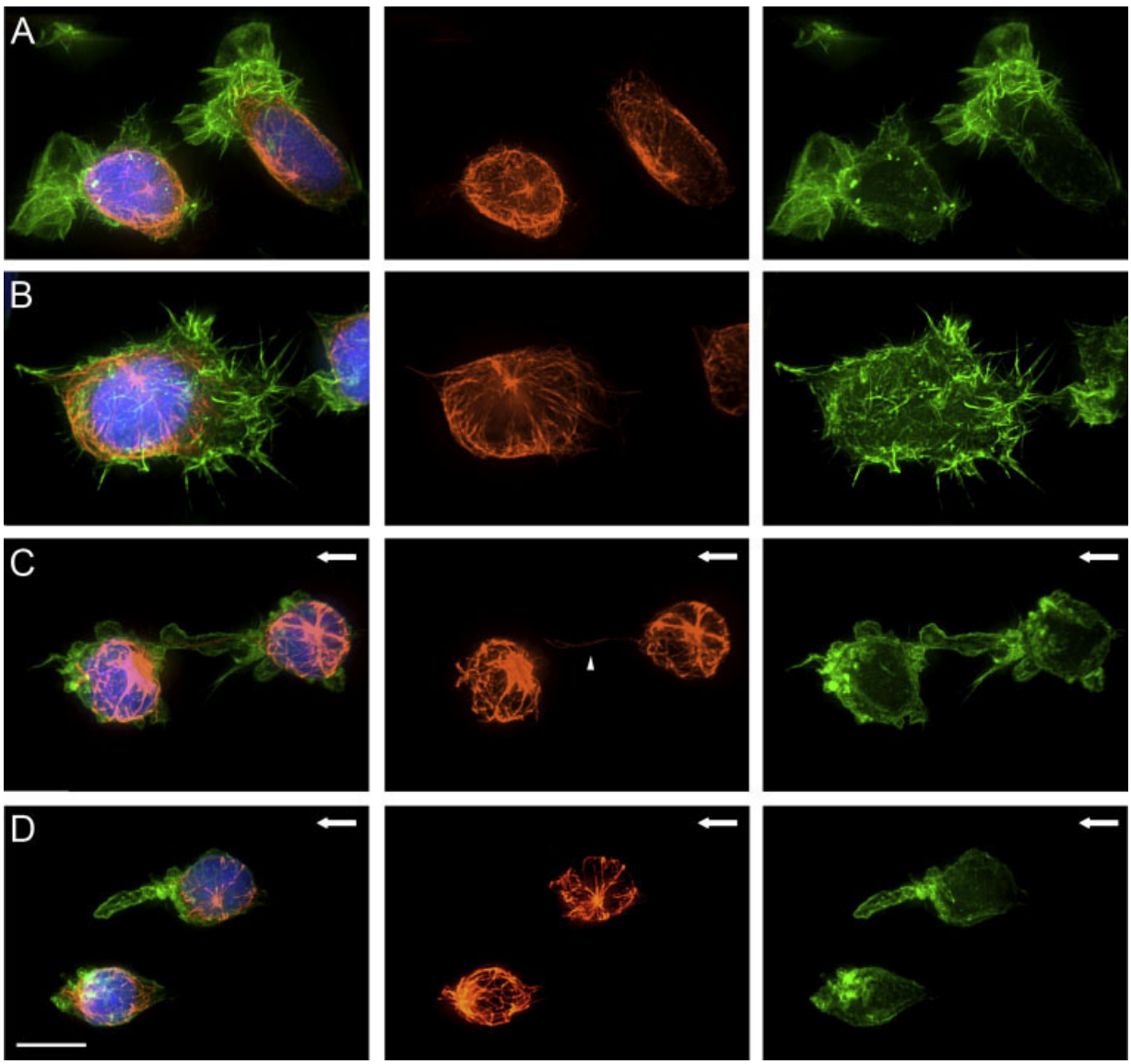

Fig. 4. Actin and tubulin localization in multiple myeloma cells exposed to shear flow. Fluorescence microscopy images of ARH-77 type A cells under flow. Cells were fixed and labeled with phalloidin-FITC (right part), anti-α-tubulin antibody (middle part) and DAPI (merge, left part). A, B: Control cells, not exposed to flow, show microtubule networks with distinct perinuclear microtubule organizing center and numerous actin-rich lamellipodia and microvilli extensions formed throughout the cell surface. C, D: Cells exposed to shear flow. The cell surface becomes smooth and free of microvilli and lamellae, and localization of FLIPs and other membrane extensions at the cell edge in the direction of flow can be seen. The FLIPs are rich in actin, located at the plasma membrane, and largely devoid of microtubules. An example of a FLIP with a single microtubule fiber is indicated by an arrowhead. Direction of flow is marked with an arrow. Scale bar is 10 μm.

"slow-retracting" cells displaying FLIPs that persist for 12–40 min (~40% of the cells). Interestingly, there were no significant differences in FLIP lifespan between cells exposed to different force levels (~5% in each duration category, 12–44 min).

Further examination of FLIP initiation time reveals that while at weaker forces (12–20 dynes/cm^2), FLIP formation shows a relatively even distribution over the experimental period, stronger forces (28–36 dynes/cm^2) induce a notable synchronization in FLIP appearance, shortly after exposure to the flow (Fig. 10). This is demonstrated in the average FLIP initiation time, ranging from 2.68 min under 36 dynes/cm^2, to 9 min under 12 dynes/cm^2.

Moreover, the "fast retracting" cells (shorter FLIP duration) also demonstrate less sensitivity to force, as more of these cells respond later to the force. Similarly, the "slow retracting" cells are more sensitive to the force applied, as more cells respond earlier (Fig. 10B). This parameter defines the two subpopulations as "fast retracting, less sensitive" and "slow retracting, highly sensitive" cells.

Discussion

In this article, we describe a unique response of MM cells to mechanical perturbation, manifested in the formation of long tubular protrusions, which we termed FLIPs. The formation of FLIPs is a shear stress-induced process, which appears to be specific to MM cells exposed to such stress (shown here for three separate MM cell lines), and was not observed in any of the other adherent cell types tested, nor in MM cells in

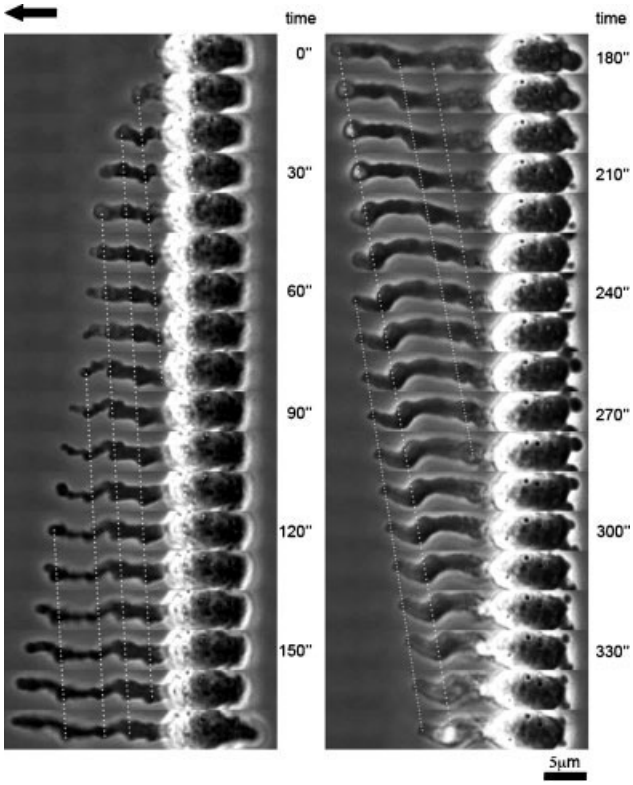

Fig. 5. Dynamics of FLIP formation and retraction. Phase-contrast images of ARH-77 type A cells under flow. Time indicates interval (in sec) after initiation of FLIP formation. The FLIP shown is elongating at its tip (left part), with concomitant slow, backwards retraction that occurs at its base (right part). Direction of flow is marked by an arrow.

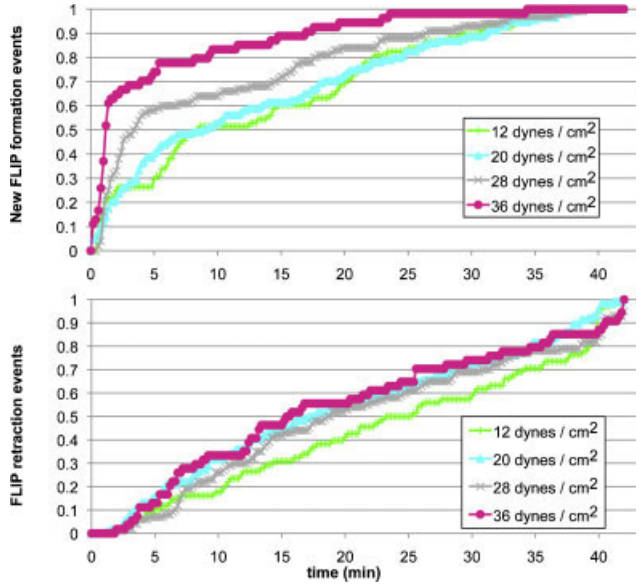

Fig. 7. FLIP extension, but not retraction, is affected by force level. ARH-77 type A cells were exposed to shear flow as indicated, time-lapse movies were taken, and FLIP formation was analyzed. At each time point, the numbers of FLIP formation and FLIP retraction events were counted. Shown here are the cumulative scores, indicated by the percentage of total numbers of FLIPs formed during 40 min of treatment for each force level. While higher levels of shear force increased the incidence of new FLIP formation, the FLIP retraction rate was not affected by changes in shear stress.

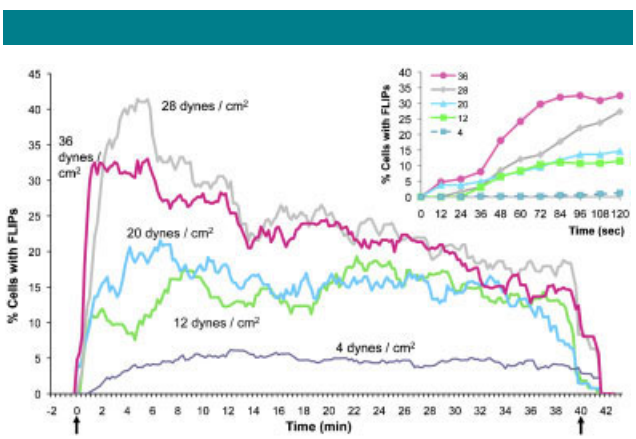

Fig. 6. Shear force level affects FLIP formation. ARH-77 type A cells were placed inside the chamber, and shear forces of 4,12, 20, 28, or 36 dynes/cm^2 were applied for 40 min. Time-lapse movies were taken, and the number of FLIP-forming cells was scored, and presented as a percentage. Black arrows indicate flow start and end times. Inset shows FLIP formation during the first 2 min after exposure to flow. It can be seen that the stronger the force, the higher the percentage of FLIP-producing cells, and the shorter the lag period.

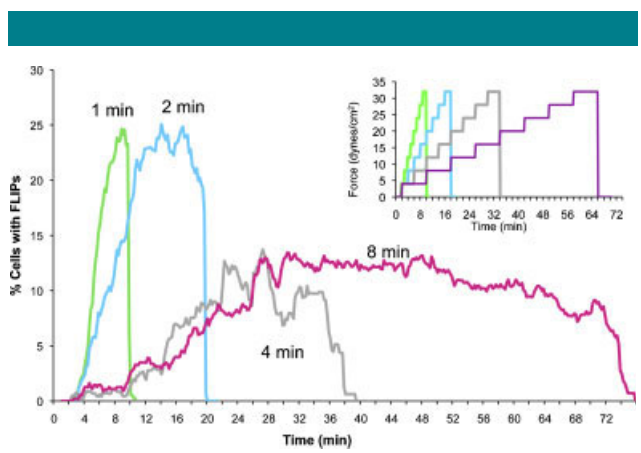

Fig. 8. FLIP suppression is induced by shear flow, yet is highly dependent on the duration, rather than the force, of the shear treatment. ARH-77 type A cells were placed inside the flow chamber. A shear force of 4 dynes/cm^2 was applied, and then increased in a stepwise fashion to 8, 12, 16, 20, 24, 28, and 32 dynes/cm^2 (see inset for force change). Each force level was applied for variable lengths of time, ranging from 1 to 8 min for each force step. Time-lapse movies were then taken, and FLIP formation was scored. It appears that the duration of exposure to flow plays a major role in the suppression of FLIP formation, as longer flow times resulted in a decrease in FLIP formation events.

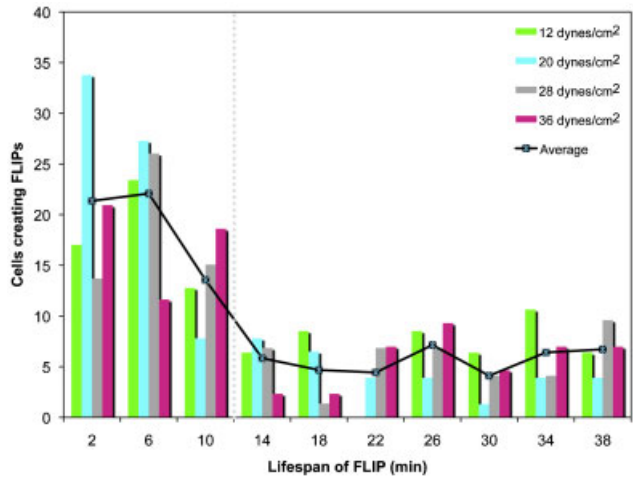

Fig. 9. Lifespan of FLIPs: Single-cell analysis of the data from Figure 6. Cells that extended FLIPs were analyzed, according to their FLIP lifespan. The population could be roughly divided into two groups, separated by the vertical dashed line: Fast-retracting cells (left) that have a maximum FLIP lifespan of 12 min, and slow-retracting cells (right). This difference is not dependent on the level of force applied.

stationary cultures. Notably, besides the formation of robust FLIPs, the MM cells stimulated by shear force underwent a major structural reorganization, manifested in their alignment in the direction of flow, and loss of filopodia and lamellipodia from the entire cell body.

Extracellular stimuli may induce membrane protrusions in various cell types, often associated with diverse cellular functions. For example, macrophages contact their targets by actively extending actin-rich protrusions, depending on Rac activity (Flannagan et al., 2010); fusion-competent myoblasts form multiple finger-like extensions which invade neighboring muscle founder cells during myoblast fusion in *Drosophila* (Sens et al., 2010); ECM and soluble factors (e.g., EGF) can induce filopodial and lamellipodial protrusions in various cell types (Hu et al., 2011; Mori et al., 2010). While these serve as examples of membrane modification by extracellular biochemical signals, biophysical cues may also trigger the formation of membrane protrusions, including the extension of FLIPs, as described in the current study.

While FLIP formation is a novel phenomenon, cellular responses to shear flow have been documented in diverse cell types. It has been shown that endothelial cells subjected to near-physiological shear undergo uniform alignment (Dewey et al., 1981; Masuda and Fujiwara, 1993; Galbraith et al., 1998), and directional migration and lamellipodial extension in the direction of flow (Dewey et al., 1981; Wojciak-Stothard and Ridley, 2003; Zaidel-Bar et al., 2005). Hematopoietic cells, which reside, at least transiently, in high-shear vascular environments, respond to flow in a variety of ways. T cells undergo dynamic shape changes during transendothelial migration, including tethering and rolling along the endothelial surfaces, firm attachment to the underlying cells, spreading on them, and trans-migration through the endothelial cell layer (Dong et al., 1999; Alon and Dustin, 2007; Stroka and Aranda-Espinoza, 2010). Platelets also go through several shape changes, including transition from a round morphology, forming multiple elongated extensions during the adhesive process under flow (Kuwahara et al., 2002). In addition, flow-induced effects were seen in other cell types, such as rolling of human bone-metastatic prostate tumor cells on endothelial cells (Dimitroff et al., 2004); transendothelial migration of melanoma cells (Slattery and Dong, 2003); increased adhesion and spreading in colon cancer cells (Kitayama et al., 1999; Burdick et al., 2003); and elongation and reorientation in osteoblasts (Liu et al., 2010). In all these cases (as well as in the present work), the response to shear flow was apparent, yet the exact cellular site where the mechanical perturbation is being sensed (e.g., dorsal cell surface, adhesion sites to the matrix) remains unclear (Cao et al., 1998; Bershadsky et al., 2003; Chen, 2008).

Similar to these shear-dependent processes, FLIP formation appears to be an active process, triggered by external force and driven by the cytoskeleton. This notion is supported by the abundance of actin filaments in the FLIP, and its tendency to undergo extension–retraction cycles under constant shear.

An interesting feature of FLIPs is the tight correlation between the amount of force applied, and both the number of FLIP-forming cells (ranging from ~5% under 4 dynes/cm^2, to ~35% under 28–36 dynes/cm^2) and the time interval between the application of force, and the average onset of FLIP extension (9 min for 12 dynes/cm^2, and 2.68 min for 36 dynes/cm^2). Time-lapse monitoring of the affected cells confirmed that different cells within the MM cell population exhibit different mechanosensing thresholds, affecting the extent and rates of FLIP formation. This increase in the number of FLIPs under strong shear is attributed to an increase in the numbers of mechano-responsive cells, while the rates of FLIP retraction, and the average lifespan of the FLIPs, remained unchanged under different levels of shear stimulation (Fig. 7).

An additional characteristic feature of the response of the cells to high-shear stimulation is the apparent adaptation of the cells to the flow, manifested in a decrease in the number of FLIP-forming cells, following lengthy exposure (about 30 min) to the flow. This finding indicates that shear-induced FLIP formation can be down-regulated by the cells, possibly by modulation of the mechanical threshold levels.

Single-cell analysis further demonstrated the heterogeneity of the cellular response to force. Increased shear forces resulted in earlier and more homogenous FLIP onset times, while under weaker forces, FLIP onset was more variable. Furthermore, the cell population could be roughly divided into two subpopulations, based upon FLIP onset and duration time: a shorter FLIP lifetime was correlated with lower sensitivity to force, as more of these cells responded later to its application, while cells demonstrating longer FLIP lifetimes responded more quickly (Fig. 10B). It is possible that variations in sensitivity to force reflect different potential adhesion sites in different cells, corresponding to the various forces encountered in their path and, in that manner, enabling each of the cells' subpopulations to adhere or extravasate at diverse locations.

The studies described above reveal the intriguing biophysical characteristics of FLIP formation, retraction, and long-term regulation; yet the physiological relevance of this structure remains elusive. In this work, we have considered several potential processes relevant to MM cell physiology that could, potentially, be relevant to FLIP formation. MM cells develop in the BM; yet they are capable of exiting the BM via the vascular system, and then homing back to BM niches throughout the body (Van Camp and Van Riet, 1998; Vande Broek et al., 2008). Thus, the process of disease dissemination includes obligatory intravasation and extravasation events, which involve major transitions in the hydrodynamic characteristics of the cellular environment. These include a transition from the relatively sessile BM niche, to the BM vasculature, to a high-shear environment in the major blood vessels, ranging from 1–10 dynes/cm^2 in venules, to 60 dynes/cm^2 and more in arterioles (Slack and Turitto, 1993). It is noteworthy that this range of shear forces is within the range that was found here to trigger FLIP formation in different populations of MM cells.

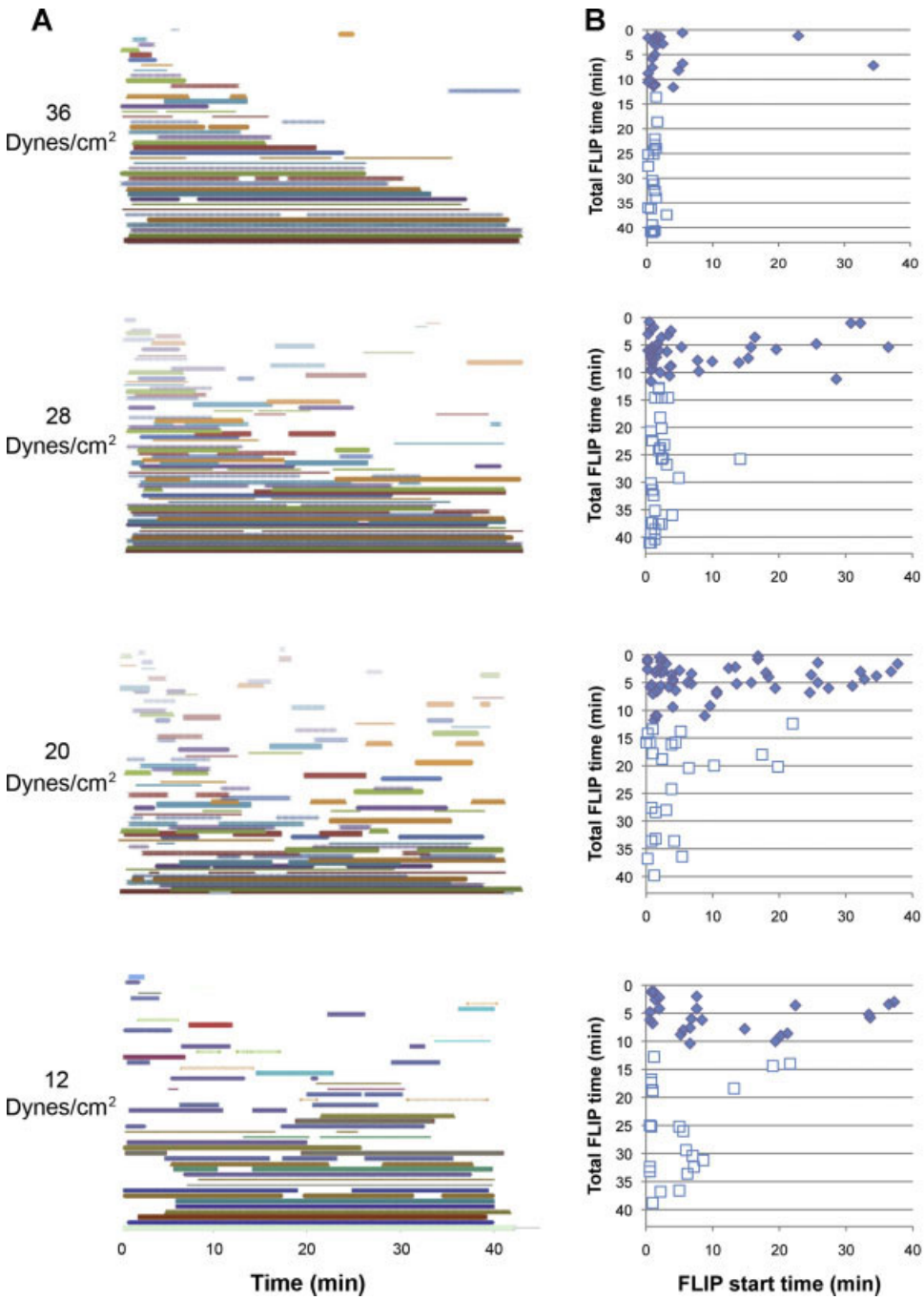

Fig. 10. The force-responding cell population can be divided into highly sensitive, slow-retracting cells, and poorly sensitive, fast-retracting cells. A: FLIP formation in individual cells for different force levels over time. Each cell is represented by a different colored line. Time, in minutes, is shown from the beginning of flow. B: Plot showing the relative initiation times of FLIP formation, as a function of FLIP lifespan under different levels of shear stress. It is shown that FLIP extension is mainly force-dependent, as strong shear force induced FLIP formation in all cells. Sensitive cells also respond to weak forces, while insensitive cells require the stimulus of strong force. The insensitive subpopulation is also fast-retracting (B, solid diamonds), whereas the FLIPs formed by the sensitive cells display longer lifespans (B, empty squares).

Interestingly, despite showing migratory capabilities in stationary cultures, ARH-77 type A cells did not appear to migrate during exposure to flow, regardless of FLIP formation or retraction. The extravasation step appears to be the most challenging one, requiring firm adhesion of the cells to the vessel wall (to withstand the shear drag forces), and migration through it. One attractive possibility that we considered was that the FLIPs produced might be instrumental in triggering a transendothelial migration process. To test this possibility, we exposed a monolayer of endothelial cells with ARH-77 cells attached to it, to shear flow, and monitored the fate and dynamics of the attached cells. As shown in Supplementary Figure 1, above, we could detect FLIP formation in such stressed, mixed cultures, as well as penetration of the MM cells into the gap between the endothelial cells and the substrate; however, we found no evidence that this transendothelial

migration was particularly enhanced in FLIP-forming cells, nor that shear flow affected this process. Another hypothesis is that FLIP formation might decrease cellular resistance to flow and thus reduce the drag forces acting on the cells, thereby increasing their retention on the vessel wall. A rough calculation of the expected flow resistance suggested that a hemispherical MM cell, covered by multiple filopodial and lamellopodial protrusions and typically several micrometers in length (as in cells residing in a stationary environment), is subjected to severalfold-higher drag forces, compared to an aligned FLIP-forming cell of the same volume. Given that MM cells display a wide range of "mechanosensitivity thresholds," it appears possible that different cells might preferentially form FLIPs, and develop more stable adhesions with blood vessels exposed to distinct levels of shear stress.

In recent years, it was established that the microenvironment plays a critical role in the development of B cell malignancies. Most studies in the field point to interactions between MM cells and cellular constituents of the microenvironment (e.g., osteoclasts, mesenchymal stromal cells) as key factors controlling the survival and proliferation of the transformed cells. Moreover, some clinical manifestations of the disease are facilitated by physical MM–microenvironment interactions; for example, the generation of lytic bone lesions by MM–osteoclast co-aggregates (Terpos et al., 2009), and the stimulation of SDF1/CXCR4-mediated cell migration (Zhang et al., 2009; Katz, 2010).

Shear stress is undoubtedly an important constituent of the microenvironment of migrating MM cells; yet no information is available with respect to its effect on these cells. Here we show, for the first time, that some MM cells are equipped with mechanism(s) to sense and respond to forces exerted by microenvironmental shear stress. Moreover, we found that different variables of the shear flow, including a wide range of forces and duration of the flow, are within the "detection capabilities" of these cells. Finally, the data described here reveal profound diversity within the MM cell population, with respect to mechanosensory responsiveness.

Acknowledgments

This work was supported by the National Institutes of Health (NIH) Common Fund Nanomedicine program (PN2 EY016586), and the NanoII project, supported by the EU FP7 program. The electron microscopy studies were conducted at the Irving and Cherna Moskowitz Center for Nano and Bio-Nano Imaging at the Weizmann Institute of Science. The authors would like to thank Helena Sabanay and Dr. Eugenia Klein from the Electron Microscopy Unit at the Weizmann Institute of Science for their help in sample preparation and examination. The authors are grateful to Barbara Morgenstern for expert editorial assistance. B.G. is the Erwin Neter Professor of Cell and Tumor Biology.

Literature Cited

Alon R, Dustin ML. 2007. Force as a facilitator of integrin conformational changes during leukocyte arrest on blood vessels and antigen-presenting cells. Immunity 26:17–27.
Bershadsky AD, Balaban NQ, Geiger B. 2003. Adhesion-dependent cell mechanosensitivity. Annu Rev Cell Dev Biol 19:677–695.
Burdick MM, McCaffery JM, Kim YS, Bochner BS, Konstantopoulos K. 2003. Colon carcinoma cell glycolipids, integrins, and other glycoproteins mediate adhesion to HUVECs under flow. Am J Physiol Cell Physiol 284:C977–C987.
Cao J, Donell B, Deaver DR, Lawrence MB, Dong C. 1998. In vitro side-view imaging technique and analysis of human T-leukemic cell adhesion to ICAM-1 in shear flow. Microvasc Res 55:124–137.
Chen CS. 2008. Mechanotransduction—A field pulling together? J Cell Sci 121:3285–3292.
Chen CS, Mrksich M, Huang S, Whitesides GM, Ingber DE. 1997. Geometric control of cell life and death. Science 276:1425–1428.
Cinamon G, Shinder V, Alon R. 2001. Shear forces promote lymphocyte migration across vascular endothelium bearing apical chemokines. Nat Immunol 2:515–522.
Cohen M, Joester D, Geiger B, Addadi L. 2004. Spatial and temporal sequence of events in cell adhesion: From molecular recognition to focal adhesion assembly. Chembiochem 5:1393–1399.
Cukierman E, Pankov R, Stevens DR, Yamada KM. 2001. Taking cell–matrix adhesions to the third dimension. Science 294:1708–1712.
Curtis A, Riehle M. 2001. Tissue engineering: The biophysical background. Phys Med Biol 46:R47–R65.
Dewey CF, Jr., Bussolari SR, Gimbrone MA, Jr., Davies PF. 1981. The dynamic response of vascular endothelial cells to fluid shear stress. J Biomech Eng 103:177–185.
Dimitroff CJ, Lechpammer M, Long-Woodward D, Kutok JL. 2004. Rolling of human bone-metastatic prostate tumor cells on human bone marrow endothelium under shear flow is mediated by E-selectin. Cancer Res 64:5261–5269.
Discher DE, Janmey P, Wang YL. 2005. Tissue cells feel and respond to the stiffness of their substrate. Science 310:1139–1143.
Discher DE, Mooney DJ, Zandstra PW. 2009. Growth factors, matrices, and forces combine and control stem cells. Science 324:1673–1677.
Dong C, Cao J, Struble EJ, Lipowsky HH. 1999. Mechanics of leukocyte deformation and adhesion to endothelium in shear flow. Ann Biomed Eng 27:298–312.
Doyle AD, Wang FW, Matsumoto K, Yamada KM. 2009. One-dimensional topography underlies three-dimensional fibrillar cell migration. J Cell Biol 184:481–490.
Engler AJ, Sen S, Sweeney HL, Discher DE. 2006. Matrix elasticity directs stem cell lineage specification. Cell 126:677–689.
Flannagan RS, Harrison RE, Yip CM, Jaqaman K, Grinstein S. 2010. Dynamic macrophage "probing" is required for the efficient capture of phagocytic targets. J Cell Biol 191:1205–1218.
Fouchard J, Mitrossilis D, Asnacios A. 2011. Acto-myosin based response to stiffness and rigidity sensing. Cell Adhes Migration 5:16–19.
Friedl P, Wolf K. 2010. Plasticity of cell migration: A multiscale tuning model. J Cell Biol 188:11–19.
Galbraith CG, Skalak R, Chien S. 1998. Shear stress induces spatial reorganization of the endothelial cell cytoskeleton. Cell Motil Cytoskeleton 40:317–330.
Geblinger D, Addadi L, Geiger B. 2010. Nano-topography sensing by osteoclasts. J Cell Sci 123:1503–1510.
Gooding RP, Bybee A, Cooke F, Little A, Marsh SG, Coelho E, Gupta D, Samson D, Apperley JF. 1999. Phenotypic and molecular analysis of six human cell lines derived from patients with plasma cell dyscrasia. Br J Haematol 106:669–681.
Heino J, Kapyla J. 2009. Cellular receptors of extracellular matrix molecules. Curr Pharm Des 15:1309–1317.
Hu J, Mukhopadhyay A, Craig AW. 2011. Transducer of Cdc42-dependent actin assembly promotes epidermal growth factor-induced cell motility and invasiveness. J Biol Chem 286:2261–2272.
Juliano R. 1996. Cooperation between soluble factors and integrin-mediated cell anchorage in the control of cell growth and differentiation. Bioessays 18:911–917.
Katz BZ. 2010. Adhesion molecules—The lifelines of multiple myeloma cells. Semin Cancer Biol 20:186–195.
Kitayama J, Nagawa H, Tsuno N, Osada T, Hatano K, Sunami E, Saito H, Muto T. 1999. Laminin mediates tethering and spreading of colon cancer cells in physiological shear flow. Br J Cancer 80:1927–1934.
Kumar S. 2010. Multiple myeloma—Current issues and controversies. Cancer Treat Rev 36 S3–S11.
Kurpinski K, Chu J, Hashi C, Li S. 2006. Anisotropic mechanosensing by mesenchymal stem cells. Proc Natl Acad Sci USA 103:16095–16100.
Kuwahara M, Sugimoto M, Tsuji S, Matsui H, Mizuno T, Miyata S, Yoshioka A. 2002. Platelet shape changes and adhesion under high shear flow. Arterioscler Thromb Vasc Biol 22:329–334.
Kyle RA, Rajkumar SV. 2004. Multiple myeloma. N Engl J Med 351:1860–1873.
Liu X, Zhang X, Lee I. 2010. A quantitative study on morphological responses of osteoblastic cells to fluid shear stress. Acta Biochim Biophys Sin (Shanghai) 42:195–201.
Ludwig H, Beksac M, Blade J, Boccadoro M, Cavenagh J, Cavo M, Dimopoulos M, Drach J, Einsele H, Facon T, Goldschmidt H, Harousseau JL, Hess U, Ketterer N, Kropff M, Mendeleeva L, Morgan G, Palumbo A, Plesner T, San Miguel J, Shpilberg O, Sondergeld P, Sonneveld P, Zweegman S. 2010. Current multiple myeloma treatment strategies with novel agents: A European perspective. Oncologist 15:6–25.
Masuda M, Fujiwara K. 1993. Morphological responses of single endothelial cells exposed to physiological levels of fluid shear stress. Front Med Biol Eng 5:79–87.
Mitchison TJ, Cramer LP. 1996. Actin-based cell motility and cell locomotion. Cell 84:371–379.
Moore SW, Roca-Cusachs P, Sheetz MP. 2010. Stretchy proteins on stretchy substrates: The important elements of integrin-mediated rigidity sensing. Dev Cell 19:194–206.
Mori T, Ono K, Kariya Y, Ogawa T, Higashi S, Miyazaki K. 2010. Laminin-3B11, a novel vascular-type laminin capable of inducing prominent lamellipodial protrusions in microvascular endothelial cells. J Biol Chem 285:35068–35078.
Nadav L, Katz BZ, Baron S, Cohen N, Naparstek E, Geiger B. 2006. The generation and regulation of functional diversity of malignant plasma cells. Cancer Res 66:8608–8616.
Nelson CM, Jean RP, Tan JL, Liu WF, Sniadecki NJ, Spector AA, Chen CS. 2005. Emergent patterns of growth controlled by multicellular form and mechanics. Proc Natl Acad Sci USA 102:11594–11599.
Papusheva E, Heisenberg CP. 2010. Spatial organization of adhesion: Force-dependent regulation and function in tissue morphogenesis. EMBO J 29:2753–2768.
Sens KL, Zhang S, Jin P, Duan R, Zhang G, Luo F, Parachini L, Chen EH. 2010. An invasive podosome-like structure promotes fusion pore formation during myoblast fusion. J Cell Biol 191:1013–1027.
Sher T, Miller KC, Deeb G, Lee K, Chanan-Khan A. 2010. Plasma cell leukaemia and other aggressive plasma cell malignancies. Br J Haematol 150:418–427.
Simon SI, Goldsmith HL. 2002. Leukocyte adhesion dynamics in shear flow. Ann Biomed Eng 30:315–332.
Slack SM, Turitto VT. 1993. Chapter 2 Fluid dynamic and hemorheologic considerations. Cardiovasc Pathol 2:11–21.
Slattery MJ, Dong C. 2003. Neutrophils influence melanoma adhesion and migration under flow conditions. Int J Cancer 106:713–722.
Spatz JP, Geiger B. 2007. Molecular engineering of cellular environments: Cell adhesion to nano-digital surfaces. Methods Cell Biol 83:89–111.
Stroka KM, Aranda-Espinoza H. 2010. A biophysical view of the interplay between mechanical forces and signaling pathways during transendothelial cell migration. FEBS J 277:1145–1158.
Terpos E, Sezer O, Croucher PI, Garcia-Sanz R, Boccadoro M, San Miguel J, Ashcroft J, Blade J, Cavo M, Delforge M, Dimopoulos MA, Facon T, Macro M, Waage A, Sonneveld P. 2009. The use of bisphosphonates in multiple myeloma: Recommendations of an expert panel on behalf of the European Myeloma Network. Ann Oncol 20:1303–1317.

Thery M, Racine V, Piel M, Pepin A, Dimitrov A, Chen Y, Sibarita JB, Bornens M. 2006. Anisotropy of cell adhesive microenvironment governs cell internal organization and orientation of polarity. Proc Natl Acad Sci USA 103:19771–19776.
Van Camp B, Van Riet I. 1998. Homing mechanisms in the biology of multiple myeloma. Verh K Acad Geneeskd Belg 60:163–194.
Van Goethem E, Poincloux R, Gauffre F, Maridonneau-Parini I, Le Cabec V. 2010. Matrix architecture dictates three-dimensional migration modes of human macrophages: Differential involvement of proteases and podosome-like structures. J Immunol 184:1049–1061.
Vande Broekl, Vanderkerken K, Van Camp B, Van Riet I. 2008. Extravasation and homing mechanisms in multiple myeloma. Clin Exp Metastasis 25:325–334.
Vogel V, Sheetz M. 2006. Local force and geometry sensing regulate cell functions. Nat Rev Mol Cell Biol 7:265–275.
Wojciak-Stothard B, Ridley AJ. 2003. Shear stress-induced endothelial cell polarization is mediated by Rho and Rac but not Cdc42 or PI 3-kinases. J Cell Biol 161:429–439.
Zaidel-Bar R, Cohen M, Addadi L, Geiger B. 2004. Hierarchical assembly of cell–matrix adhesion complexes. Biochem Soc Trans 32:416–420.
Zaidel-Bar R, Kam Z, Geiger B. 2005. Polarized downregulation of the paxillin-p130CAS-Rac1 pathway induced by shear flow. J Cell Sci 118:3997–4007.
Zamir E, Katz BZ, Aota S, Yamada KM, Geiger B, Kam Z. 1999. Molecular diversity of cell–matrix adhesions. J Cell Sci 112:1655–1669.
Zhang J, Sattler M, Tonon G, Grabher C, Lababidi S, Zimmerhackl A, Raab MS, Vallet S, Zhou Y, Cartron MA, Hideshima T, Tai YT, Chauhan D, Anderson KC, Podar K. 2009. Targeting angiogenesis via a c-Myc/hypoxia-inducible factor-1alpha-dependent pathway in multiple myeloma. Cancer Res 69:5082–5090.